Am J Clin Exp Immunol 2025;14(3):145-156
www.ajcei.us /ISSN:2164-7712/AJCEI0160434

Original Article

Diagnostic value of CD20 combined with CD138 positive expression in patients with chronic endometritis

Jingyi Yi[1], Peiru Zhang[1], Lvxuan Chen[1], Shuqiang Chu[2], Luhong Li[1]

[1]Department of Obstetrics and Gynecology, The Second Affiliated Hospital of Fujian Medical University, Quanzhou 362000, Fujian, China; [2]Department of Pathology, The Second Affiliated Hospital of Fujian Medical University, Quanzhou 362000, Fujian, China

Received September 9, 2024; Accepted May 3, 2025; Epub June 15, 2025; Published June 30, 2025

Abstract: Background: This study aims to evaluate the diagnostic value of CD138 and CD20 immunohistochemical staining in chronic endometritis (CE). Methods: A total of 131 patients with reproductive needs, treated at the Second Affiliated Hospital of Fujian Medical University between August 2020 and July 2021, were enrolled. Patients were divided into a CD138-positive group (n=91) and a CD138-negative group (n=40). All participants provided informed consent and underwent hysteroscopic examination using an Olympus 30° scope, following standard operating procedures. Lesion shape and size were recorded in detail. CE diagnosis was based on hysteroscopic findings of patchy bleeding and confirmed by endometrial biopsy of suspicious areas. Biopsy tissues were subjected to immunohistochemical staining for CD138 and CD20. Expression levels were assessed under low-power and high-power magnification (Original magnification: ×400. Scale bar: 20 μm). Results: CD20 expression differed significantly between the CD138-positive and CD138-negative groups (χ^2=45.440.160, P<0.05). The kappa coefficient for agreement between CD20 and CD138 was 0.530 (95% CI 2.072-4.684, P<0.05). A significant difference in CD20 expression at ×400 magnification was also observed between the two groups (χ^2=12.520, P<0.05), with a kappa coefficient of 0.300(95% CI 0.594-1.164, P<0.05). The area under the ROC curve (AUC) for CD20 in predicting CE was 0.732, and 0.665 for CD20 at ×400 magnification, indicating reliable diagnostic performance for both. Conclusions: In patients with chronic endometritis, both the positive expression of CD20 and its high-level expression at ×400 magnification provide valuable diagnostic indicators, demonstrating better diagnostic utility.

Keywords: Chronic endometritis, hysteroscopy, CD138, CD20, influencing factors

Introduction

Chronic endometritis (CE) is a prevalent chronic inflammatory disorder in gynecology and has garnered increasing attention in recent years [1]. This condition is associated with impaired endometrial receptivity, leading to reduced pregnancy rates in both natural conception and assisted reproductive technology (ART), and contributes to adverse outcomes such as recurrent implantation failure, recurrent miscarriage, and preterm birth [2, 3]. Recent studies have demonstrated that the uterine cavity is not sterile [4]. Advances in sequencing techniques, such as 16S rRNA analysis, have revealed the presence of a normal microbiota dominated by Lactobacillus in the endometrium of healthy women. Unlike acute endometritis, which arises from acute infections, CE is now understood to stem from dysbiosis of the uterine microbiota rather than overt infections. However, the precise pathogenic mechanisms remain incompletely elucidated. Infection during embryo transfer and implantation can lead to embryo damage, transfer failure, and then lead to serious adverse pregnancy events such as abortion. Infections during embryo transfer or implantation may damage the embryo, cause implantation failure, and ultimately result in severe adverse outcomes such as miscarriage. To explore the pathogenic causes of CE from a clinical perspective, it is partly due to the presence of foreign bodies or pathological structural changes in the endometrium [5, 6]. CE often presents asymptomatically, with only a minority of patients exhibiting atypical symptoms such as increased leukorrhea, chronic pelvic pain, or abnormal uterine bleeding [7, 8]. This asymp-

https://doi.org/10.62347/LIHI3143

tomatic nature contributes to frequent clinical underdiagnosis, and the true prevalence of CE in reproductive-age women remains poorly defined. Additionally, the lack of standardized diagnostic criteria has led to significant variability in reported CE prevalence across studies, ranging from 2.8% to 56.8% in infertile populations and 14.0% to 67.5% in those with recurrent implantation failure. Abnormal infiltration of inflammatory cells in the endometrium is a hallmark of CE [9]. The primary diagnostic criterion for CE is the identification of plasma cells within the endometrial stroma. The primary diagnostic criterion for CE is the identification of plasma cells within the endometrial stroma. First described in 1907, infiltration of endometrial stromal plasma cells (ESPC) has been the gold standard for CE diagnosis since its initial identification. Conventional hematoxylin and eosin (HE) staining has largely been supplanted by immunohistochemistry (IHC) due to its low specificity for detecting plasma cells. In recent years, researchers have proposed the use of syndecan-1 (CD138), a transmembrane heparan sulfate proteoglycan, as a specific marker for plasma cells. This has led to its adoption in immunohistochemical analysis for CE diagnosis. CD138 immunohistochemistry specifically identifies these proteoglycans in ESPC, providing definitive pathological evidence for CE diagnosis.

In addition to plasma cell infiltration, CE is characterized by significant lymphocytic infiltration, including large lymphoid aggregates and occasional lymphoid follicle formation. The B-lymphocyte marker CD20 aids in distinguishing physiological endometrial lymphocytic infiltration from inflammatory infiltration in endometritis. CD20-positive B lymphocytes are critical in CE pathogenesis. Immunohistochemical staining of these cells aids in confirming CE diagnosis, particularly when plasma cells are scarce or poorly recognized. In a 1996 study by O Tawfik et al. [10], 25 cases of CE and 35 control endometrial biopsies were analyzed. Morphological analysis revealed significant plasma cell infiltration in all CE patients, but no specific lymphocyte infiltration was observed. Neutrophil infiltration was noted in 90% of cases. Additional nonspecific histological features include lymphatic aggregation, interstitial edema, hemorrhage, necrosis, and cystic glandular dilation in the endometrium of CE patients. Immunohistochemical analysis using CD20 antibodies revealed that CD20-positive B lymphocytes comprised <2% of immune cells in control patients (mean: <2 cells/high-power field [HPF]). In contrast, numerous CD20-positive lymphocytes were observed in CE patient endometria. Semiquantitative analysis demonstrated a 50-fold increase in CD20-positive cells in CE patients compared to controls. These cells were predominantly localized in subepithelial and periglandular aggregates[11]. These findings suggest that CD20-positive B lymphocytes may play a critical role in CE pathogenesis. This study aims to evaluate hysteroscopic findings and analyze CD138 and CD20 immunohistochemical staining in CE patients. The goal is to assess their diagnostic utility for CE, thereby improving clinical diagnostic accuracy and reducing missed diagnoses.

Materials and methods

General information

A total of 131 patients with fertility needs from the Second Affiliated Hospital of Fujian Medical University were enrolled as the study population between August 2020 and July 2021. Written informed consent was obtained voluntarily from all participants. All participants underwent hysteroscopy and endometrial biopsy during the proliferative phase of the menstrual cycle (3-7 days after menstruation). CD138 immunohistochemistry was used as the diagnostic criterion for CE. The CE incidence rate was calculated, and the diagnostic utility of CD20 for CE was evaluated. Comparisons were made of CD20's diagnostic performance across different CE subgroups. Patients were divided into CD138+ (n=91) and CD138- (n=40) groups based on CD138 immunohistochemical results. Demographic and clinical data were collected for both groups. Statistical comparisons were performed to evaluate associations between CD20 expression levels and demographic/clinical characteristics in both groups.

Inclusion criteria

Patients with reproductive needs were included if they met the following criteria: Complete clinical data were available. Hysteroscopy and endometrial biopsy were scheduled. Endometrial tissue obtained during biopsy was analyzed using immunohistochemical staining for CD138 and CD20. All procedures were con-

ducted during the proliferative phase of the menstrual cycle (Days 3-7 after menstruation).

Exclusion criteria

Exclusion criteria included the following: Current or recent urogenital infection or antibiotic use within the past month. Active bleeding, significant endometrial thickening (>10 mm), uterine congenital anomalies, or intrauterine contraceptive device placement. Pathological findings of non-proliferative endometrium (e.g., atrophic endometrium), endometrial hyperplasia, endometrial cancer, or other non-benign lesions. Pregnancy or retained fetal products. History of hysteroscopic surgery or use of hormonal medications (e.g., combined oral contraceptives) within the past 3 months. Poor ovarian reserve (e.g., AFC <5 follicles or AMH <1.0 ng/mL).

Main reagents

Reagents and materials used in this study included the following.

Primary antibodies: CD138 antibody (immunohistochemistry): Clone M115, Product No. MAB-0200. CD20 antibody (immunohistochemistry): Clone L26, Product No. KIT-0001. All antibodies were sourced from Fuzhou Maixin Biotechnology Development Co., Ltd. (Fuzhou, China).

Immunohistochemical kits: Max Vision TMH-RP Kit (ready-to-use, rat/rabbit): Product No. KIT-5020. Antigen Retrieval Buffer (EDTA-based): Product No. MVS-0099. Enhanced DAB Chromogen Kit: Product No. DAB-2031. Endogenous Peroxidase Blocking Solution: Product No. SPKIT-A2. All kits were purchased from Fuzhou Maixin Biotechnology Development Co., Ltd.

Additional reagents: Hematoxylin Staining Solution: Product No. CTS-1090 (Fuzhou Maixin). PBS Buffer (phosphate): Product No. PBS-0060 (Fuzhou Maixin). Van Clear (environmental transparent agent): Product No. H-H0101 (Zhonghuitong Scientific Research Service Center, Qingdao, China).

Common laboratory materials: Absolute ethanol, 95% ethanol, 85% ethanol, distilled water, and sealing gum were obtained from the Department of Pathology at our institution.

Main instruments and equipment

Instruments and equipment used in this study included the following.

Tissue processing and microscopy: Paraffin microtome (Model HM325). Biological microscope (Model BX53, Sony Corporation, Japan). Pathological imaging system (ICX452AQ, Semefi, UK).

Sterilization and incubation equipment: Stainless steel autoclave, incubator, and oven (Olympus Corporation, Japan), provided by the Department of Pathology.

Endoscopic and surgical equipment: Endoscopic system (EVIS EXERAIII CV-190, Olympus Corporation, Japan). Uterine dilation system and hysteroscopic surgical instruments, provided by the hospital's operating room.

All equipment was sourced from either the Department of Pathology or the operating room at our institution.

Experimental methods and procedures: endometrial biopsy

Endometrial biopsy procedures were performed as follows.

Preoperative preparation: Written informed consent was obtained from patients for hysteroscopy and endometrial biopsy. Preoperative evaluations were conducted, including clinical history review and relevant laboratory tests.

Procedure details: Hysteroscopy was performed by a senior attending physician (with expertise in hysteroscopy) and an assistant. A 30° Olympus hysteroscope (outer sheath diameter: 6.5 mm; endoscope diameter: 3.0 mm) was used. The uterine cavity was distended using 0.9% sodium chloride solution at a pressure of 80-110 mmHg. The following anatomical regions were systematically examined: cervical canal, uterine fundus, bilateral uterine angles, fallopian tube ostia, and anterior/posterior/lateral walls of the uterine cavity. Detailed documentation of lesion morphology and size was recorded.

Diagnosis and biopsy: CE was diagnosed based on hysteroscopic findings such as polypoid lesions, interstitial edema, or flaky hemorrhagic spots. Endometrial biopsy was performed at

suspicious sites. For patients with endometrial polyps ≥0.5 cm, polyp tissue was collected for histopathological analysis.

All procedures were conducted under sterile conditions in the operating room.

CD138 and CD20 immunohistochemistry

Immunohistochemical staining for CD138 and CD20 was performed as follows.

Tissue processing: Endometrial tissue samples were fixed in 10% neutral buffered formalin, dehydrated via ethanol gradient, and embedded in paraffin to produce 4-μm-thick sections.

Antigen retrieval and staining protocol is as follows.

Deparaffinization and rehydration: Slides were deparaffinized in xylene and rehydrated through graded ethanol (100%, 95%, 85%) followed by distilled water. Endogenous peroxidase activity was blocked with 1% hydrogen peroxide for 10 minutes at room temperature.

Antigen retrieval: Sections were immersed in EDTA buffer (pH 9.0) and heated in a boiling water bath for 20 minutes. Cooled to room temperature and rinsed with PBS (3×3 minutes).

Primary antibody incubation: Slides were incubated with CD138 (Clone M115, 1:100 dilution) and CD20 (Clone L26, 1:200 dilution) antibodies separately at room temperature for 60 minutes. Washed with PBS (3×3 minutes).

Secondary antibody and chromogen: Envision polymer (sheep anti-mouse/rabbit IgG, 1:200) was applied for 15 minutes at room temperature. DAB substrate was added for 3-5 minutes to visualize staining. Counterstained with hematoxylin for 10-30 seconds, followed by PBS rinsing to bluing.

Post-staining steps: Slides were dehydrated through ethanol series, cleared with xylene, and mounted with mounting medium.

Result interpretation: Two board-certified pathologists independently reviewed the slides. CD138+ cells (≥10 plasma cells/high-power field) were considered diagnostic for CE. CD20 staining intensity and distribution were semi-quantitatively scored (0-3+).

All steps were performed under standardized laboratory conditions.

Observation indices and diagnostic criteria

The following criteria were used to evaluate immunohistochemical staining results.

CD138 staining interpretation is as follows.

ESPC identification: Endothelial spindle-shaped plasma cells (ESPCs) exhibited strong membranous CD138 staining (brownish-yellow) and weak cytoplasmic staining.

Nuclear features included a thick, radially arranged chromatin pattern along the nuclear membrane, forming a wheel-like structure. Cytoplasm displayed basophilic staining.

CE diagnosis: CE was diagnosed if either of the following criteria were met: Presence of plasma cells in CD138-stained sections [≥5 ESPCs per ×400 magnification high-power field (HPF)]. Non-CE (NCE): <5 ESPCs per ×400 magnification HPF or absence of ESPCs.

CD20 staining interpretation: Strong CD20 positivity indicates the presence of oval, polygonal, or grid-shaped cells with abundant immature lymphocytes. The diagnostic criteria for CD20 positivity are defined as ≥5 ESPCs (Epithelioid Stromal Plasma Cells) per ×400 magnification HPF, while CD20 negativity is characterized by <5 ESPCs per ×400 magnification HPF or the absence of ESPCs.

Pathologist review: Two board-certified pathologists independently evaluated the slides. Discrepancies were resolved through consensus, with a third pathologist providing final arbitration if necessary.

All criteria were applied in accordance with standardized immunohistochemical scoring guidelines.

Statistical analysis

The statistical analyses were performed using the Statistical Package for the Social Sciences version 29.0 (SPSS Inc., Chicago, IL, USA). Non-normally distributed metric variables were analyzed by the Kruskal-Wallis test and Mann-Whitney U-test. The mean surface areas of the endometriotic implants between the same

Table 1. Comparison of general conditions between the two groups

Items	CD138+ group(n=91)	CD138- group(n=40)	t/χ^2	P
Age (years)	31.37±3.93	30.83±4.28	0.704	0.476
Height (cm)	166.90±6.69	168.90±8.12	1.436	0.153
Weight (kg)	67.05±12.22	68.35±11.00	0.575	0.566
Abdominal circumference (cm)	80.08±3.22	80.78±3.10	1.153	0.225
BMI (kg/m^2)	23.97±3.55	23.92±3.06	0.086	0.931
Fallopian_Tube_Obstruction			2.527	0.283
No	63 (69.2%)	33 (82.5%)		
Unilateral	21 (23.1%)	5 (12.5%)		
Bilateral	7 (7.7%)	2 (5.0%)		
Single_or_Multiple_polyp(s)			2.856	0.24
No	33 (36.3%)	18 (45.0%)		
Single polyp	12 (13.2%)	8 (20.0%)		
Multiple polyps	46 (50.5%)	14 (35.0%)		
Menstrual_changes			4.152	0.042
Normal	68 (74.7%)	22 (55.0%)		
Abnormal	23 (25.3%)	18 (45.0%)		
Abnormal_Vaginal_Bleeding			0.921	0.337
No	85 (93.4%)	39 (97.5%)		
Yes	6 (6.6%)	1 (2.5%)		
CS_History			0.496	0.781
0	80 (87.9%)	35 (87.5%)		
1	10 (11.0%)	5 (12.5%)		
2	1 (1.1%)	0 (0.0%)		
History_of_Abortion			7.818	0.05
0	62 (68.1%)	21 (52.5%)		
1	23 (25.3%)	11 (27.5%)		
2	6 (6.6%)	6 (15.0%)		
3	0 (0.0%)	2 (5.0%)		
History_of_Vaginal_Delivery			0.499	0.779
0	75 (82.4%)	34 (85.0%)		
1	15 (16.5%)	6 (15.0%)		
2	1 (1.1%)	0 (0.0%)		
Basic FSH (IU/L)	16.75±8.16	18.88±7.72	1.396	0.165
Thickness of foundation inner membrane (mm)	4.47±4.02	4.80±3.70	0.439	0.662

group (before and after the medical treatment) were analyzed by Wilcoxon's signed-rank test. $P<0.05$ was considered statistically significant. Values were expressed as mean ± standard deviation, unless stated otherwise.

Results

Comparison of baseline characteristics between CD138+ group and CD138- group

Baseline characteristics of the CD138+ and CD138- groups are summarized in **Table 1**. No significant differences were observed between the groups in age (t=0.704, P=0.476), height (t=1.436, P=0.153), weight (t=0.575, P=0.566), abdominal circumference (t=1.153, P=0.225), body mass index (BMI) (t=0.086, P=0.931), basal follicle-stimulating hormone (FSH) levels (t=1.396, P=0.165), or basal endometrial thickness (t=0.439, P=0.662). All *P*-values exceeded 0.05, indicating no statistical significance.

CD20 immunohistochemical subgroup results

Subgroup analysis based on CD138 immunohistochemical results revealed statistically

Table 2. Results of CD20 immunohistochemical subgroup

Items	CD138+ group (n=91)	CD138- group (n=40)	χ^2	P
CD20+	89 (97.8%)	20 (50.0%)	45.440	<0.05
CD20-	2 (9.1%)	20 (50.0%)		

Table 3. Kappa coefficient results of consistency between CD20 & CD138

Index	Kappa value	P	95% CI (lower limit)	95% CI (upper limit)
CD20 & CD138	0.530	<0.05	2.072	4.684

Table 4. Positive results of CD38 and CD20 at ×400 magnification

Items	CD138+ group (n=91)	CD138- group (n=40)	χ^2	P
CD20 at ×400 magnification	62 (68.1%)	14 (35.0%)	12.520	<0.05

significant differences between groups (χ^2= 45.440, P<0.05, **Table 2**).

CD20 and CD138 kappa coefficient results

The agreement between CD20 and CD138 staining was assessed using the kappa coefficient. A moderate level of consistency was observed (κ=0.530, 95% CI: 7.938-108.39, P< 0.05, **Table 3**).

Comparison of CD20 at ×400 magnification positive expression between CD138+ and CD138- groups

CD20 expression at ×400 magnification was compared between CD138+ and CD138- groups. Significant differences were identified (χ^2=12.520, P<0.05, **Table 4**).

Concordance between CD20 at ×400 magnification and CD138

The concordance between CD20 staining at ×400 magnification and CD138 expression was evaluated using the kappa statistic. A moderate level of agreement was observed (κ= 0.300, 95% CI: 0.594-1.164, P<0.05, **Table 5**).

ROC curve analysis of CD20 and CD20 at ×400 magnification for CE prediction

Receiver operating characteristic (ROC) curve analysis demonstrated that CD20 had an AUC of 0.733, while CD20 at ×400 magnification yielded an AUC of 0.661 for predicting CE. Both markers showed moderate predictive reliability, with CD-20 exhibiting a larger AUC (**Figure 1**).

Immunohistochemical staining results (envision method)

Figure 2 illustrates the expression of CD20 and CD138 in cases 1-4.

Case 1: At ×200 magnification (**Figure 2A**), scattered CD20+ B cells with positive membrane staining were observed in the endometrial stroma. At ×400 magnification (**Figure 2B**), cellular details were clear, with positive signals concentrated on the cell membrane. For CD138 staining, ×200 magnification (**Figure 2C**) revealed a small number of CD138+ plasma cells in the stroma, displaying brown-yellow positive reactions in the cell membrane and cytoplasm. At ×400 magnification (**Figure 2D**), typical plasma cell morphology was evident, with eccentric nuclei and distinct cytoplasmic staining.

Case 2: CD20 staining (**Figure 2E**, **2F**) showed scattered CD20+ B cells in the endometrial stroma with positive membrane expression; cell density was slightly lower at ×400 magnification (**Figure 2F**) compared to Case 1. CD138 staining (**Figure 2G**, **2H**) identified focal plasma cells at ×200 magnification (**Figure 2G**), with clear cytoplasmic positive signals at ×400 magnification (**Figure 2H**).

Case 3: CD20 staining (**Figure 2I**, **2J**) demonstrated a significant reduction in $CD20^+$ B cells, with no clearly positive cells detected at either ×200 or ×400 magnification. CD138 staining (**Figure 2K**, **2L**) also showed no $CD138^+$ plasma cells, with stromal cells exhibiting negative reactions.

Case 4: CD20 (**Figure 2M**, **2N**) and CD138 (**Figure 2O**, **2P**) staining results were consistent with Case 3, with no positive cells detected in the endometrial stroma.

Figure 3 further validated the immunophenotype of representative cases.

Table 5. Kappa coefficient results of CD20, ×400 to CD138

Items	Kappa value	P	95% CI (lower limit)	95% CI (upper limit)
CD20 at ×400 magnification & CD138	0.300	<0.05	0.594	1.164

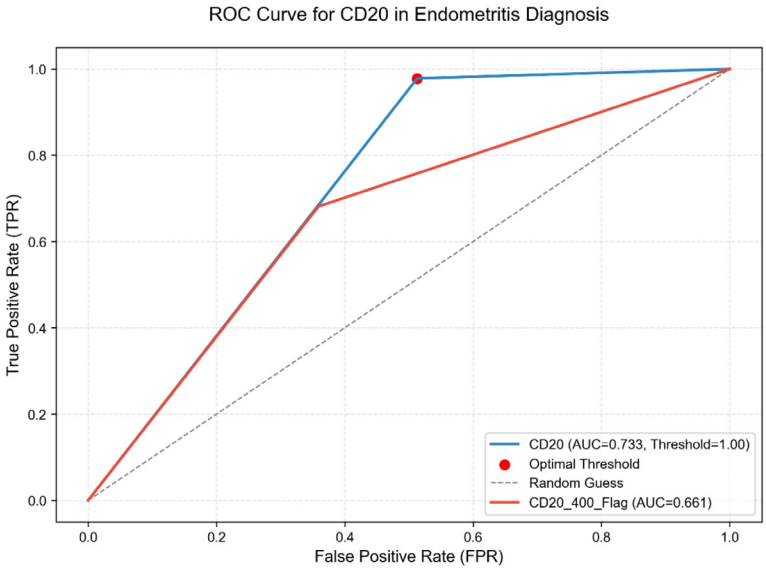

Figure 1. ROC curve of positive predictive value of CD20 and CD20, ×400

CD20 staining (**Figure 3A**, ×400) showed scattered B cells in the endometrial stroma with specific positive membrane expression, consistent with the B-cell immunophenotype.

CD138 staining (**Figure 3B**, ×400) demonstrated characteristic positive signals in the cell membrane and cytoplasm of plasma cells in corresponding regions, indicating plasma cell infiltration.

HE staining results

Figure 4 shows histological observations.

Cases 1 and 2: At ×200 magnification (**Figure 4A**, **4C**), scattered round cells with eccentric nuclei and basophilic cytoplasm-morphologically consistent with plasma cells-were observed in the endometrial stroma. At ×400 magnification (**Figure 4B**, **4D**), plasma cell details were distinct, with prominent perinuclear hofs, indicating minimal plasma cell infiltration in the stroma.

Cases 3 and 4: No typical plasma cell morphology was identified in the endometrial stroma at either ×200 or ×400 magnification (**Figure 4E-H**). The stroma primarily consisted of fibroblasts and a small number of lymphocytes, with no evident inflammatory cell infiltration.

Discussion

CE is defined as localized inflammation of the endometrium, primarily characterized by interstitial edema [12, 13]. In some patients, the density of interstitial cells increases, accompanied by the infiltration of plasma cells into the endometrium. The diagnostic hallmark of CE is the presence of plasma cell infiltration within the endometrial stroma. Pathological examination reveals that plasma cells exhibit larger cell bodies, smaller nuclei (typically eccentric), basophilic cytoplasm, and heterochromatin arranged in a spoke-like pattern within the nucleus. These morphological features resemble those of endometrial stromal fibroblasts and monocytes [14-16]. During the secretory phase, endometrial surface edema and the physiological increase in stromal cell density can complicate the distinction between stromal cells and plasma cells, further increasing the risk of misidentification. The diagnosis of CE is highly susceptible to subjective factors at multiple stages, from specimen collection to pathological interpretation. This subjectivity reduces the accuracy of plasma cell identification within the endometrial stroma, leading to a high rate of missed diagnoses [17, 18].

The accurate acquisition of endometrial specimens is crucial for the pathological diagnosis of CE [19-21]. Currently, endometrial tissue is typically collected through diagnostic curettage or hysteroscopy [22-24]. Diagnostic curettage may introduce cervical canal tissue into the samples, complicating the differentiation between cervical and endometrial plasma cell infiltration. Additionally, this method carries a risk of endometrial injury, making it less favorable for patients with reproductive needs [25-

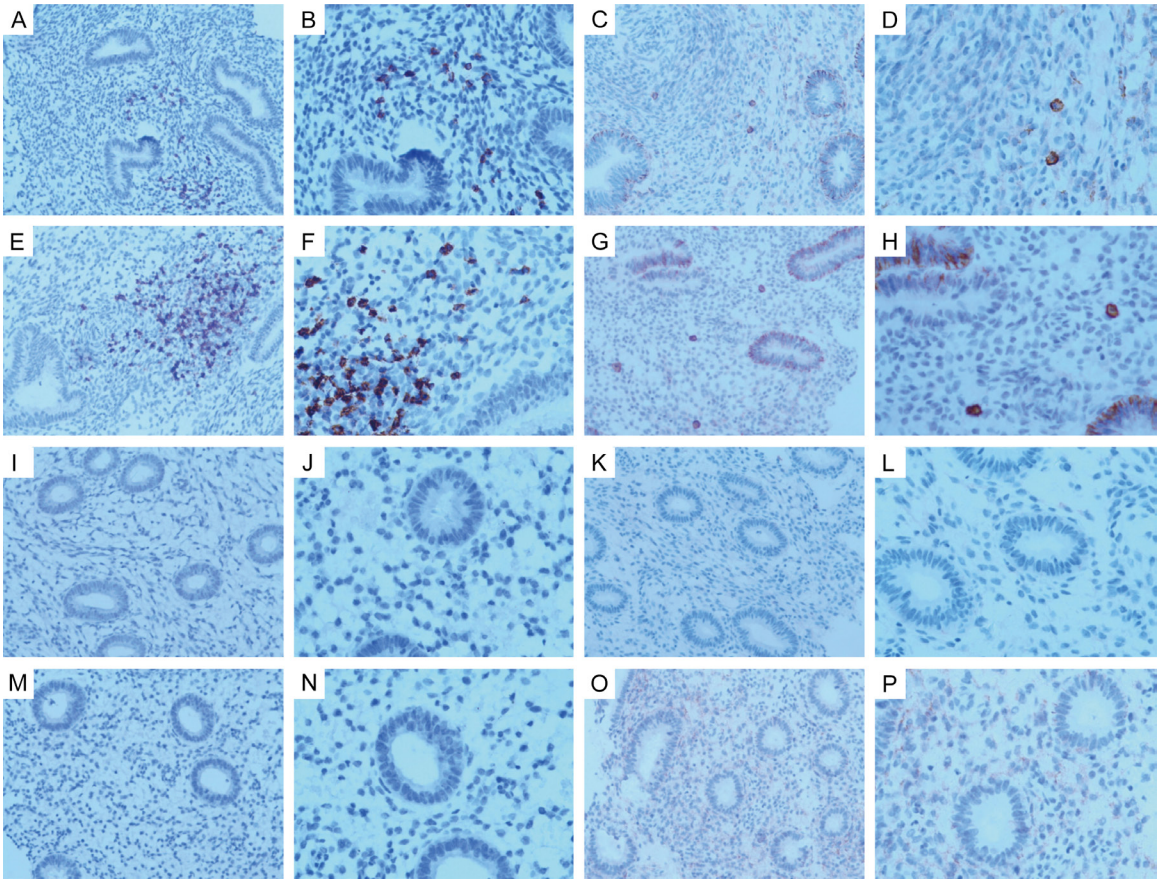

Figure 2. Immunohistochemical results of CD20 and CD138 at ×200 and ×400 magnification, respectively. (A) is the CD20 image of Case 1 under a microscope at ×200 magnification, and a small number of B lymphocytes can be seen. (B) is the CD20 image of Case 1 under a microscope at ×400 magnification, and a small number of B lymphocytes can be seen. (C) is the CD138 image of Case 1 under a microscope at ×200 magnification, and a small number of plasma cells can be seen. (D) is the CD138 image of Case 1 under a microscope at ×400 magnification, and a small number of plasma cells can be seen. (E) is the CD20 image of Case 2 under a microscope at ×200 magnification, and a small number of B lymphocytes can be seen. (F) is the CD20 image of Case 2 under a microscope at ×400 magnification, and a small number of B lymphocytes can be seen. (G) is the CD138 image of Case 2 under a microscope at ×200 magnification, and a small number of plasma cells can be seen. (H) is the CD138 image of Case 2 under a microscope at ×400 magnification, and a small number of plasma cells can be seen. (I) is the CD20 image of Case 3 under a microscope at ×200 magnification, and no lymphocytes are visible. (J) is the CD20 image of Case 3 under a microscope at ×400 magnification, and no lymphocytes are visible. (K) is the CD138 image of Case 3 under a microscope at ×200 magnification, and no plasma cells are visible. (L) is the CD138 image of Case 3 under a microscope at ×400 magnification, and no plasma cells are visible. (M) is the CD20 image of Case 4 under a microscope at ×200 magnification, and no lymphocytes are visible. (N) is the CD20 image of Case 4 under a microscope at ×400 magnification, and no lymphocytes are visible. (O) is the CD138 image of Case 4 under a microscope at ×200 magnification, and no plasma cells are visible. (P) is the CD138 image of Case 4 under a microscope at ×400 magnification, and no plasma cells are visible. Original magnification ×200, with Scale bar of 50 μm; Original magnification ×400, with Scale bar of 100 μm.

27]. Hysteroscopy, widely adopted in clinical practice, especially in hospitals at or above Level II, offers significant advantages as a minimally invasive technique. Not only does it aid in treating gynecological conditions, but it also enhances diagnostic accuracy [28]. In clinical settings, hysteroscopy serves two primary functions: conducting a comprehensive visual inspection of the uterine cavity to identify lesion locations and characteristics, and collecting targeted tissue samples for pathological analysis. Routine biopsies are also performed on typical physiological and anatomical sites within the uterine cavity to reduce the likelihood of missed diagnoses of CE [29-31]. Several studies have compared hysteroscopy with methods like vaginal ultrasound and diagnostic curettage [12, 32], revealing that hysteroscopy

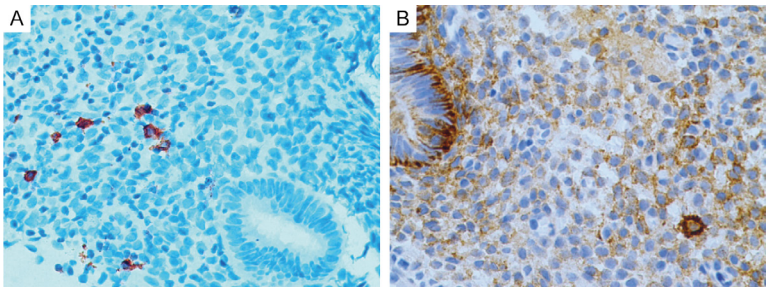

Figure 3. Immunohistochemical results of CD20 at ×400 and CD138 at ×400 magnification, respectively. (A) is the staining result of CD20 at ×400 magnification. A small number of B cells are found in the stroma of endometrium, showing positive expression of cell membrane, envision method. (B) is the result of CD138 at ×400 magnification. Individual plasma cells are found in the stroma of endometrium, showing positive expression of cell membrane, envision method. Original magnification ×200, with Scale bar of 50 μm; Original magnification ×400, with Scale bar of 100 μm.

offers superior diagnostic sensitivity and specificity for CE. For instance, Cremasco et al. [33] coined the term "strawberry sign" to describe the appearance of focal or scattered white punctate glands in the congested endometrium, which are prone to bleeding upon hysteroscopic examination. This technique also allows for the identification of endometrial micro-polyps, typically less than 1 mm in diameter. Hysteroscopy leverages magnification principles to enhance visualization of the uterine cavity, facilitating precise sampling of affected tissues. This reduces the risk of missed diagnoses and minimizes endometrial damage, thereby increasing detection rates and improving diagnostic outcomes. Experts like Cidnelli have proposed specific hysteroscopic criteria for diagnosing CE, including tiny polyps, focal hyperemia, interstitial edema, an "endometrial strawberry" appearance, and endometrial bleeding points [34-36]. Endometrial interstitial edema, characterized by irregular thickening of the endometrium with or without slight pale elevation, poses challenges for microscopic diagnosis. A recent case-control study identified several independent risk factors for CE, including diffuse and focal congestion, punctate congestion, interstitial vascular exposure, and micro-polyps. While hysteroscopy improves diagnostic capabilities, its effectiveness can be influenced by factors such as the clinician's experience and the type of uterine distension medium used. Currently, hysteroscopy is not considered a standard diagnostic tool for CE due to its lower sensitivity and specificity compared to immunohistochemical staining. A recent retrospective study reported hysteroscopy sensitivities and specificities of 59.3% and 69.7%, respectively, which are notably lower than those achieved with immunohistochemical methods [37]. Thus, while hysteroscopy is valuable as an adjunctive diagnostic tool, it cannotreplace immunohistochemical staining for definitive diagnosis.

This study reveals that the absence or scarcity of plasma cells in the endometrium does not definitively rule out the presence of CE, as plasma cells may occasionally appear in healthy endometrial tissue. The hallmark pathological feature of CE is the infiltration of plasma cells into the endometrial stroma. Additionally, CE is associated with a significant increase in lymphocyte numbers. Under normal conditions, the lymphocytes in the endometrial stroma are predominantly T cells, with B lymphocytes comprising only approximately 1% of the total leukocyte population. These B lymphocytes are typically restricted to lymphoid aggregates in the basal layer of the endometrium. However, in cases of CE, abnormal proliferation of B lymphocytes occurs, leading to their aberrant distribution in the endometrial stroma outside the lymphoid aggregates. Occasionally, these cells may also be observed in the epithelium and glandular cavities. In this study, the kappa coefficient measuring the agreement between CD20 and CD138 was 0.530 (95% CI: 2.197-5.269), indicating moderate consistency. The area under the receiver operating characteristic (ROC) curve (AUC) for CD20 at ×400 magnification was 0.866, demonstrating a reliable predictive value for CE. Among 20 patients who tested negative for CD138 but positive for CD20, 18 were highly suspected of having CE based on hysteroscopic findings and clinical symptoms, signs, and manifestations. These 18 patients were treated with doxycycline (200 mg/day for 14 days). Post-treatment, some patients underwent hysteroscopic reevaluation and immunohistochemical analysis, which revealed a significant reduction in CD20-positive cells under high-power microscopy.

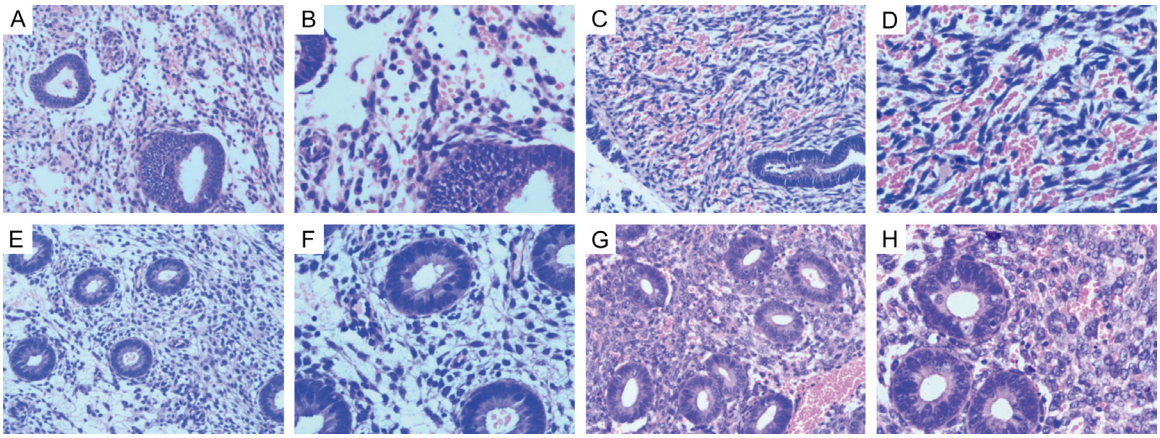

Figure 4. HE staining results at ×200 and ×400 magnification, respectively. (A) shows a small number of plasma cells visible in the endometrial stroma under HE staining at ×200 magnification for Case 1; (B) shows a small number of plasma cells visible in the endometrial stroma under HE staining at ×400 magnification for Case 1; (C) shows a small number of plasma cells visible in the endometrial stroma under HE staining at ×200 magnification for Case 2; (D) shows a small number of plasma cells visible in the endometrial stroma under HE staining at ×400 magnification for Case 2; (E) shows no plasma cells in the endometrial stroma under HE staining at ×200 magnification for Case 3; (F) shows no plasma cells in the endometrial stroma under HE staining at ×400 magnification for Case 3; (G) shows no plasma cells in the endometrial stroma under HE staining at ×200 magnification for Case 4; (H) shows no plasma cells in the endometrial stroma under HE staining at ×400 magnification for Case 4. Original magnification ×200, with Scale bar of 50 μm; Original magnification ×400, with Scale bar of 100 μm.

After six months of follow-up, eight of the 18 patients achieved pregnancy, yielding a pregnancy rate of 44.4%.

This study aimed to explore the relationship between CE and CD20 expression. Our findings confirm that CD20 has significant diagnostic potential for CE. However, due to the small sample size, the study has certain limitations. Future research could investigate the thresholds of CD20 (×400) and CD138/HPF levels that reliably diagnose CE, thereby offering an alternative diagnostic approach for clinical practice. To enhance the reliability of clinical applications, subsequent studies should expand the dataset and include multicenter patient cohorts.

Acknowledgements

This study was supported by the 2018 Quanzhou Science and Technology Project Fund Plan (the 2th batch) (No. 2018N021S).

Written informed consent was obtained from all patients.

Disclosure of conflict of interest

None.

Address correspondence to: Luhong Li, Department of Obstetrics and Gynecology, The Second Affiliated Hospital of Fujian Medical University, Quanzhou 362000, Fujian, China. E-mail: liluhong20101212@163.com

References

[1] de Holanda AGB, da Silva Leite J, Consalter A, da Silva KVGC, Dos Santos Batista BP, Fonseca ABM, Brandao FZ and Ferreira AMR. Expression of interleukins 6 and 10 and population of inflammatory cells in the equine endometrium: diagnostic implications. Mol Biol Rep 2019; 46: 2485-2491.

[2] Bonavida B. Cross-talk cell signaling between anti-CD20 antibodies and nitric oxide donors. Crit Rev Oncog 2020; 25: 291-300.

[3] Prica A and Crump M. Improving CD20 antibody therapy: obinutuzumab in lymphoproliferative disorders. Leuk Lymphoma 2019; 60: 573-582.

[4] Mikhaleva LM, Boltovskaya MN, Mikhalev SA, Babichenko II and Vandysheva RA. Endometrial dysfunction caused by chronic endometritis: clinical and morphological aspects. Arkh Patol 2017; 79: 22-29.

[5] Herlihy NS, Klimczak AM, Titus S, Scott C, Hanson BM, Kim JK, Seli E and Scott RT. The role of endometrial staining for CD138 as a marker of chronic endometritis in predicting live birth. J Assist Reprod Genet 2022; 39: 473-479.

[6] Palaiologou M, Delladetsima I and Tiniakos D. CD138 (syndecan-1) expression in health and disease. Histol Histopathol 2014; 29: 177-189.
[7] Couchman JR. Syndecan-1 (CD138), carcinomas and EMT. Int J Mol Sci 2021; 22: 4227.
[8] Sheta M and Götte M. Syndecan-1 (CD138) as a pathogenesis factor and therapeutic target in breast cancer. Curr Med Chem 2021; 28: 5066-5083.
[9] Cicinelli E, Matteo M, Tinelli R, Lepera A, Alfonso R, Indraccolo U, Marrocchella S, Greco P and Resta L. Prevalence of chronic endometritis in repeated unexplained implantation failure and the IVF success rate after antibiotic therapy. Hum Reprod 2015; 30: 323-30.
[10] Tawfik O, Venuti S, Brown S and Collins J. Immunohistochemical characterization of leukocytic subpopulations in chronic endometritis. Infect Dis Obstet Gynecol 1996; 4: 287-293.
[11] Ellinidi VN, Khromov-Borisov NN, Feoktistov AA, Lyamina AV and Kalinina NM. CD20+B lymphocytes, a highly informative biomarker for early diagnosis of chronic endometritis. Medical Immunology (Russia) 2019; 21: 451-456.
[12] Bansal R, Kimlinger T, Gyotoku KA, Smith M, Rajkumar V and Kumar S. Impact of CD138 magnetic bead-based positive selection on bone marrow plasma cell surface markers. Clin Lymphoma Myeloma Leuk 2021; 21: e48-e51.
[13] Barksdale B and Leith CP. CD138+ carcinocythemia mimicking plasma cell leukemia by flow cytometry. Blood 2020; 136: 1698.
[14] Gharbaran R. Advances in the molecular functions of syndecan-1 (SDC1/CD138) in the pathogenesis of malignancies. Crit Rev Oncol Hematol 2015; 94: 1-17.
[15] Liu L, Takeda K and Akkoyunlu M. Disease stage-specific pathogenicity of CD138 (Syndecan 1)-expressing T cells in systemic lupus erythematosus. Front Immunol 2020; 11: 1569.
[16] Li Y, Xu S, Yu S, Huang C, Lin S, Chen W, Mo M, Lian R, Diao L, Ding L and Zeng Y. Diagnosis of chronic endometritis: how many $CD138^+$ cells/HPF in endometrial stroma affect pregnancy outcome of infertile women? Am J Reprod Immunol 2021; 85: e13369.
[17] Moreno L, Perez C, Zabaleta A, Manrique I, Alignani D, Ajona D, Blanco L, Lasa M, Maiso P, Rodriguez I, Garate S, Jelinek T, Segura V, Moreno C, Merino J, Rodriguez-Otero P, Panizo C, Prosper F, San-Miguel JF and Paiva B. The mechanism of action of the anti-CD38 monoclonal antibody isatuximab in multiple myeloma. Clin Cancer Res 2019; 25: 3176-3187.
[18] Glaría E and Valledor AF. Roles of CD38 in the immune response to infection. Cells 2020; 9: 228.
[19] Ng HHM, Lee RY, Goh S, Tay ISY, Lim X, Lee B, Chew V, Li H, Tan B, Lim S, Lim JCT, Au B, Loh JJH, Saraf S, Connolly JE, Loh T, Leow WQ, Lee JJX, Toh HC, Malavasi F, Lee SY, Chow P, Newell EW, Choo SP, Tai D, Yeong J and Lim TKH. Immunohistochemical scoring of CD38 in the tumor microenvironment predicts responsiveness to anti-PD-1/PD-L1 immunotherapy in hepatocellular carcinoma. J Immunother Cancer 2020; 8: e000987.
[20] Payandeh Z, Bahrami AA, Hoseinpoor R, Mortazavi Y, Rajabibazl M, Rahimpour A, Taromchi AH and Khalil S. The applications of anti-CD20 antibodies to treat various B cells disorders. Biomed Pharmacother 2019; 109: 2415-2426.
[21] Houot R, Levy R, Cartron G and Armand P. Could anti-CD20 therapy jeopardise the efficacy of a SARS-CoV-2 vaccine? Eur J Cancer 2020; 136: 4-6.
[22] Gelfand JM, Cree BAC and Hauser SL. Ocrelizumab and other $CD20^+$ B-cell-depleting therapies in multiple sclerosis. Neurotherapeutics 2017; 14: 835-841.
[23] Chen Q, Yuan S, Sun H and Peng L. $CD3^+CD20^+$ T cells and their roles in human diseases. Hum Immunol 2019; 80: 191-194.
[24] Pavlasova G and Mraz M. The regulation and function of CD20: an "enigma" of B-cell biology and targeted therapy. Haematologica 2020; 105: 1494-1506.
[25] Sun LL, Ellerman D, Mathieu M, Hristopoulos M, Chen X, Li Y, Yan X, Clark R, Reyes A, Stefanich E, Mai E, Young J, Johnson C, Huseni M, Wang X, Chen Y, Wang P, Wang H, Dybdal N, Chu YW, Chiorazzi N, Scheer JM, Junttila T, Totpal K, Dennis MS and Ebens AJ. Anti-CD20/CD3 T cell-dependent bispecific antibody for the treatment of B cell malignancies. Sci Transl Med 2015; 7: 287ra270.
[26] Bacac M, Colombetti S, Herter S, Sam J, Perro M, Chen S, Bianchi R, Richard M, Schoenle A, Nicolini V, Diggelmann S, Limani F, Schlenker R, Hüsser T, Richter W, Bray-French K, Hinton H, Giusti AM, Freimoser-Grundschober A, Lariviere L, Neumann C, Klein C and Umaña P. CD20-TCB with obinutuzumab pretreatment as next-generation treatment of hematologic malignancies. Clin Cancer Res 2018; 24: 4785-4797.
[27] Huang Y, Chen S, Wei R, Guo X, Yang X, Cao Q, Yang Y and Yun J. CD20-positive extranodal NK/T cell lymphoma: clinicopathologic and prognostic features. Virchows Arch 2020; 477: 873-883.

[28] Sharman JP. Targeting CD20: teaching an old dog new tricks. Hematology Am Soc Hematol Educ Program 2019; 2019: 273-278.
[29] Akhmetzyanova I, McCarron MJ, Parekh S, Chesi M, Bergsagel PL and Fooksman DR. Dynamic CD138 surface expression regulates switch between myeloma growth and dissemination. Leukemia 2020; 34: 245-256.
[30] Liu L and Akkoyunlu M. Circulating CD138 enhances disease progression by augmenting autoreactive antibody production in a mouse model of systemic lupus erythematosus. J Biol Chem 2021; 297: 101053.
[31] Uchimido R, Schmidt EP and Shapiro NI. The glycocalyx: a novel diagnostic and therapeutic target in sepsis. Crit Care 2019; 23: 16.
[32] Wu D, Zhang P, Li F, Shen Y, Chen H, Feng Y, He A and Wang F. CD138- multiple myeloma cells express high level of CHK1 which correlated to overall survival in MM patient. Aging (Albany NY) 2020; 12: 23067-23081.
[33] Cremasco F, Menietti E, Speziale D, Sam J, Sammicheli S, Richard M, Varol A, Klein C, Umana P, Bacac M, Colombetti S and Perro M. Cross-linking of T cell to B cell lymphoma by the T cell bispecific antibody CD20-TCB induces IFNγ/CXCL10-dependent peripheral T cell recruitment in humanized murine model. PLoS One 2021; 16: e0241091.
[34] Shuai W and Li S. CD138- plasma cell myeloma. Blood 2019; 134: 906.
[35] Kind S, Kluth M, Hube-Magg C, Möller K, Makrypidi-Fraune G, Lutz F, Lennartz M, Rico SD, Schlomm T, Heinzer H, Höflmayer D, Weidemann S, Uhlig R, Huland H, Graefen M, Bernreuther C, Tsourlakis MC, Minner S, Dum D, Hinsch A, Lübke AM, Simon R, Sauter G, Marx A and Polonski A. Increased cytoplasmic CD138 expression is associated with aggressive characteristics in prostate cancer and is an independent predictor for biochemical recurrence. Biomed Res Int 2020; 2020: 5845374.
[36] Handra-Luca A. CD138/syndecan-1 in pancreatic solid and pseudopapillary neoplasms. J Clin Pathol 2019; 72: 186.
[37] Santos MAO and Lima MM. CD20 role in pathophysiology of Hodgkin's disease. Rev Assoc Med Bras (1992) 2017; 63: 810-813.